Electronic and vibrational properties of initial-stage oxidation products on Si(111)-(7×7)

Sung-Hoon Lee and Myung-Ho Kang
Department of Physics, Pohang University of Science and Technology, Pohang 790-784, Korea
(Received 11 June 1999)

Chemisorption of O_2 molecules on the adatom site of Si(111)-(7×7) has been studied by density-functional theory calculations for all possible dissociation configurations. Structures possessing an oxygen atom on top of the Si adatom are all found to be metastable and account well for the metastable electronic and vibrational spectra observed in previous experiments, while structures with only oxygen atoms inserted into the adatom back bonds appear quite stable. The present structural models therefore are all compatible with either the metastable or the stable O_2 reactions products found in this system. The calculated decay pathways of the metastable structures provide additional informations useful for identifying the experimental metastable structures.

I. INTRODUCTION

Chemisorption of oxygen molecules on the Si(111)-(7×7) surface has been studied extensively as a model for the initial-stage oxidation of the surface.[1] The dissociation of adsorbed O_2 molecules is an essential step toward the surface oxidation, but the detailed procedure and the structures of the resulting oxidation products are yet to be verified. Moreover, there have been experimental suggestions of a possibility of molecularly chemisorbed O_2 species on Si(111)-(7×7). This O_2 molecular precursor model was introduced to explain the metastable spectral features, which disappear at about 400 K, found in x-ray and ultraviolet photoelectron spectroscopy (XPS and UPS) (Refs. 2 and 3) and vibrational electron energy loss spectroscopy (EELS).[4–6] Recent scanning tunneling microscopy (STM) studies also ascribed the observed oxygen-induced bright[7,8] and dark[9] images to chemisorbed O_2 molecular states. Despite many studies,[10–23] however, there have been no direct structural evidences of the proposed O_2 molecular precursors on Si(111)-(7×7).

Recent density-functional theory (DFT) calculations[24] shed light on this system by providing quantitative structural models for the initial-stage oxidation of the Si(111)-(7×7) surface. The calculations demonstrated that (i) a single O_2 molecule adsorbed on the most reactive Si adatom site is unstable and dissociates directly without energy barrier, and (ii) the resulting atomic-oxygen products explain quantitatively the stable and metastable EELS and UPS features. This result provides no theoretical ground for the concept of O_2 molecular precursors on Si(111)-(7×7), in agreement with a recent Cs^+ reactive scattering experiments, which failed to detect outcoming $CsO_2{}^+$ ions.[25] The dissociative chemisorption models discussed in Ref. 24 are energetically sound and very useful to explain the experimental spectral features, but they are valid only for the very initial stage of oxidation process since derived from the reaction of a single O_2 molecule at the surface. In the experimental conditions many other oxidation states are possible by additional O_2 reactions, thus it is desirable to study multiply oxidized states further, which is the purpose of the present work.

In this paper, we present the results of DFT calculations for all dissociative oxidation states of the Si adatom site that can be generated by multiple O_2 reactions on Si(111)-(7×7). We have determined the equilibrium structures and analyzed their electronic and vibrational properties in comparison with measured UPS and EELS spectra. This extended work will generalize the result of Ref. 24. The remainder of this paper is organized as follows. Sec. II describes the details of our calculation methods. In Sec. III A we describe the oxidation model structures and their adsorption energetics. Their electronic and vibrational properties are presented in Sec. III B and Sec. III C, by which the structural origin of the experimental spectra can be identified. Section III D deals with the decay pathways of the metastable structures. A summary of this work is given in Sec. IV.

II. COMPUTATIONAL DETAILS

The Si(111)-(7×7) surface has three kinds of reactive adsorption sites (i.e., adatom, restatom, and corner hole sites),[26] and the adatom site was found to be the most reactive with O_2 molecules:[10–13] the UPS peak corresponding to the adatom dangling-bond state is readily quenched, and the oxygen-induced changes in STM images occur primarily on the adatom site. In the present study, therefore, we focus on the oxidation of the adatom site and simulate the local adatom geometry of the Si(111)-(7×7) surface by a periodic slab geometry with a computationally feasible (4×2) surface unit cell (see Fig. 1): Each slab contains eight layers of Si atoms. On each side of the slab, two adatoms are added, and one of the two restatom dangling bonds is saturated by a hydrogen atom in order to maintain the same population ratio of adatoms and restatoms as the (7×7) surface.[27] This surface was found to be a good approximation of the (7×7) surface in previous DFT calculations for the study of hydrogen diffusion.[28]

Figure 2 displays the oxidation models considered in the present study. These models are based on a dissociative O_2 chemisorption picture.[24,25,29] The name of each model reflects well its atomic-oxygen bonding configuration: Here, ''ad'' denotes an O atom adsorbed on top of the Si adatom, and ''ins×n'' means that n O atoms are singly inserted into

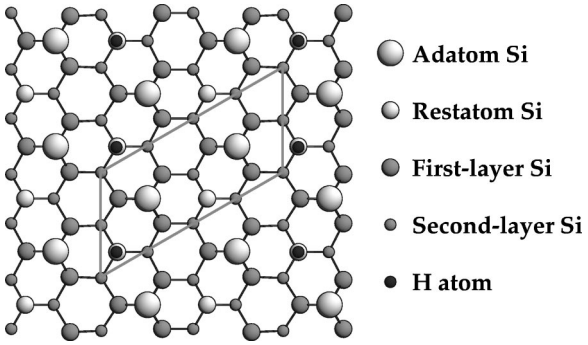

FIG. 1. (4×2) surface unit cell used for the present study. One of the two restatoms in a unit cell is saturated by a H atom to maintain the same population ratio of adatoms and restatoms as the (7×7) surface.

n Si adatom backbonds. As was demonstrated in Ref. 24, a single O_2 adsorption can result in the ad-ins or ins$\times2$ structure. An additional O_2 adsorption would lead to the ad-ins $\times3$ structure. If one O atom of the adsorbed O_2 molecule can be pushed away during the reaction, the ad, ins, ad-ins $\times2$, or ins$\times3$ structures would be possible. The possibility of such abstractive interactions of O_2 is not clear yet,[30] thus we safely included those structures in our consideration. Therefore the models given in Fig. 2 cover all possible dissociative oxidation configurations up to two successive O_2

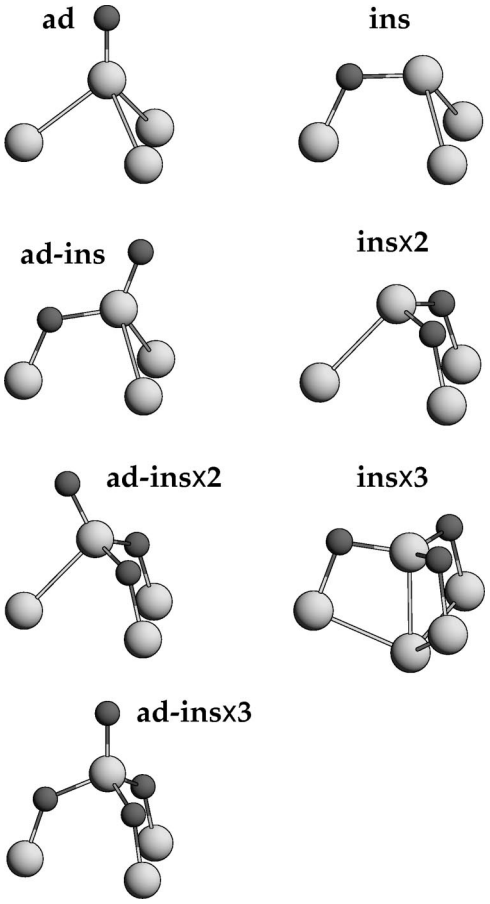

FIG. 2. Adsorption models considered in this study. The large and small circles represent Si and O atoms, respectively. The optimized structural parameters for the models are given in Table II.

TABLE I. Convergence test for the adsorption energy of the ins$\times2$ structure. Here, $E_{\rm cut}$ is the plane-wave basis cutoff, $N_{\mathbf{k}}$ is the number of $\mathbf{k}$ points in the (4×2) surface Brillouin zone, and $N_{\rm layer}$ represents the slab thickness of the Si substrate.

$E_{\rm cut}$ (Ry)	$N_{\mathbf{k}}$	$N_{\rm layer}$	$E_{\rm ads}$ (eV)
20	2	8	7.59
25	2	8	7.52
20	8	8	7.61
20	2	12	7.63

adsorption on the adatom site.

We carried out DFT calculations within the generalized gradient approximation proposed by Perdew, Burke, and Ernzerhof.[31] We used norm-conserving pseudopotentials[32–34] for Si and H atoms and ultrasoft pseudopotentials[35,36] for O atoms. The electronic wave functions were expanded in a plane-wave basis with a cutoff energy of 20 Ry. We used two $\mathbf{k}$ points in the (4×2) surface Brillouin zone for the $\mathbf{k}$-space integration. The positions of all atoms, except the innermost two Si layers held at their bulk positions, were relaxed until all the residual force components are within 0.05 eV/Å.

For a reference, we calculated the equilibrium bond length, vibration frequency, and binding energy of the free O_2 molecule in the spin-triplet ground state: The calculated values, 1.24 Å, 0.21 eV, and 6.3 eV, respectively are compared well with the experimental values, 1.21 Å, 0.20 eV, and 5.2 eV. We also tested the convergence of our slab calculations with respect to the used parameters. Table I shows the result obtained for a representative adsorption model that involves two O atoms in adatom backbonds (i.e., the ins $\times2$ model in Fig. 2). Here the adsorption energy was calculated by

$$E_{\rm ads}=-\left(E_{\rm tot}^{\rm model}-E_{\rm tot}^{\rm clean}-\frac{1}{2}E_{\rm tot}^{\rm O_2}\times N_{\rm O}\right), \qquad (1)$$

where $E_{\rm tot}^{\rm model}$, $E_{\rm tot}^{\rm clean}$, and $E_{\rm tot}^{\rm O_2}$ are the total energies of the model surface, the clean surface, and the free O_2 molecule, respectively, and $N_{\rm O}$ is the number of O atoms involved in the model. As shown in Table I, the calculated adsorption energy is converged well within 0.1 eV, and the involved structural changes are negligible.

III. RESULTS

A. Optimized structures and energetics

In Table II we display the optimized structural parameters of the models shown in Fig. 2. Noticeable features are as follows: (i) The Si-O(ad) bond lengths are almost identical in all ad-ins$\times n$ ($n=0$, 1, 2, and 3) structures, and the values are similar to the bond length of free SiO molecules (1.54 Å). (ii) The Si-O(ins)-Si bond angles are somewhat smaller than that of the crystalline SiO_2 (e.g., 144° for α-quartz) and get closer to the crystalline value as the number of backbond oxidation increases. One exception is the ins$\times3$ structure, which will be discussed shortly. (iii) In the ad-ins$\times n$ structures, the vertical position of the Si restatom is significantly lowered compared to the clean surface. The formation of a

TABLE II. Optimized structural parameters. Here, d is the bond length of the Si-O(ad) unit. For the Si-O(ins)-Si unit, d_1 (d_2) is the bond length between the O atom and the Si adatom (the first-layer Si atom), and φ is the bond angle of the Si-O-Si. The last column shows the variation of the vertical position of the restatom from the clean surface.

Model	Si-O(ad) d (Å)	Si-O-Si d_1 (Å)	Si-O-Si d_2 (Å)	Si-O-Si φ	Restatom ΔZ (Å)
ad	1.56				−0.80
ad-ins	1.56	1.72	1.69	123°	−0.71
ad-ins×2	1.56	1.72	1.68	127°	−0.57
ad-ins×3	1.57	1.72	1.66	133°	−0.42
ins		1.72	1.73	117°	−0.00
ins×2		1.71	1.72	123°	−0.00
ins×3		1.65	1.77	102°	−0.01

strong Si-O(ad) bond requires a large charge transfer from the restatom to the adatom site, which in turn drives the inward relaxation of the restatom for an electronic energy gain via a stabilizing sp^2 rehybridization.

Adsorption energies of the model structures are compared in Table III. For an O atom, the ad structure is energetically less favored (by 1.32 eV) than the ins structure. Similarly, the ad-ins and ad-ins×2 structures are also less favored than their stable counterparts, the ins×2 and ins×3 structures. That is, the O(ad) species are always metastable relative to the O(ins) species. It is also noticeable that multiply oxidized models have in general adsorption energies larger than the sum of the adsorption energies of their constituent models, i.e., for example, $E_{\rm ads}(\text{ad-ins}) = E_{\rm ads}(\text{ad}) + E_{\rm ads}(\text{ins}) + 0.31$ eV.

The ins×3 structure deserves some explanation. In this structure a large inward relaxation of the Si adatom results in the Si-O-Si angle of 102°, contrasting to the usual suggestion that the insertion of three oxygen atoms into the adatom backbonds would induce a protrusion of the Si adatom.[23] In fact, we found such a locally stable structure with the Si-O-Si angle of 127° (denoted by ins×3*), but it is less stable by 0.2 eV than the ins×3. The activation barrier for the ins×3* to ins×3 transition is as low as 0.2 eV, thus the ins×3* can easily transform into the ins×3 structure.

B. Projected density of states of oxygen 2p orbitals

In order to resolve the origin of the oxygen-induced UPS peaks, we have calculated density of states projected on O $2p$ orbitals. The projected density of states (PDOS) of an atomic orbital ϕ_α was calculated by

$$D_\alpha(\epsilon) = \sum_{\mathbf{k}n} |\langle \phi_\alpha | \psi_{\mathbf{k}n} \rangle|^2 \delta(\epsilon - \epsilon_{\mathbf{k}n}), \tag{2}$$

where $\psi_{\mathbf{k}n}$ and $\epsilon_{\mathbf{k}n}$ are the Kohn-Sham wave function and the corresponding eigenvalue, and the summation is over the first Brillouin zone and all bands. The δ function was replaced with a Gaussian of width 0.2 eV. For this calculation, norm-conserving pseudopotentials were used for O atoms with a plane-wave basis cutoff of 40 Ry.

TABLE III. Calculated oxygen adsorption energies. The values are given with respect to the free molecular state.

Model	$E_{\rm ads}$ (eV)	$E_{\rm ads}$ (eV/O)
ad	2.32	2.32
ins	3.64	3.64
ad-ins	6.27	3.14
ins×2	7.59	3.79
ad-ins×2	10.36	3.45
ins×3	11.57	3.86
ad-ins×3	14.37	3.59

We show the PDOS of the O $2p$ orbitals in Figs. 3 and 4 in comparison with experiments. The UPS spectra obtained by Höfer *et al.*[2] are shown schematically in the top panel of the figures. There, the low-binding 2.1 and 3.9 eV peaks were found to disappear by ~400 K annealing, while the other three peaks at 6–11 eV increased by the annealing. The data also show the polarization dependence of the peaks. We note in particular that the metastable 3.9 (2.1) eV peak was prominent by p-polarized (s-polarized) light.

The calculated PDOS shows that the binding energies of O $2p$ orbitals depend largely on the local bonding configurations, i.e., O(ad) atoms and O(ins) atoms produce clearly distinct binding energy spectra: The binding energy of O(ad) $2p$ ranges over 0–4 eV, while that of O(ins) $2p$ over 3.5–10 eV. Accordingly, the comparison of the PDOS and UPS data indicates that the O(ad) atoms can be ascribed to the origin of the metastable UPS peaks, while the O(ins) atoms to the stable UPS peaks. In addition, the orbital characters of the PDOS peaks account well for the polarization dependence of the metastable UPS peaks: The PDOS for O(ad) atoms exhibits two prominent peaks separated by ~2 eV, the higher binding peak being due to the p_z orbital and the lower to the nonbonding p_x and p_y orbitals. According to the symmetry selection rules for UPS measurements,[2] a p_z ($p_{x,y}$) orbital is predominantly observable for p-polarized (s-polarized) light. Thus the higher (lower) binding peak in the O(ad) PDOS should be prominent by p-polarized (s-polarized) light, which is in good agreement with the experimental observation.[2]

Our calculations tend to underestimate the binding energies of the O $2p$ orbitals by 1–2 eV compared to experimental values, as seen in Figs. 3 and 4. This underestimation can be regarded as one of the general tendencies of DFT calculations: Blase *et al.*[37] found that DFT calculations of the H/Si(111)-(1×1) surface underestimate the binding energies of hydrogen-induced surface states by 0.5–0.8 eV compared to experiments, and that the extent of underbinding depends on the degree of localization of the states. Therefore a larger underestimation of the binding energy is expected for the more localized O $2p$ orbitals.

C. Vibration spectra

We now discuss the calculated vibration spectra of the atomic oxidation models. The local vibration modes of each model structure were determined within the harmonic approximation by solving the general eigenvalue problem,

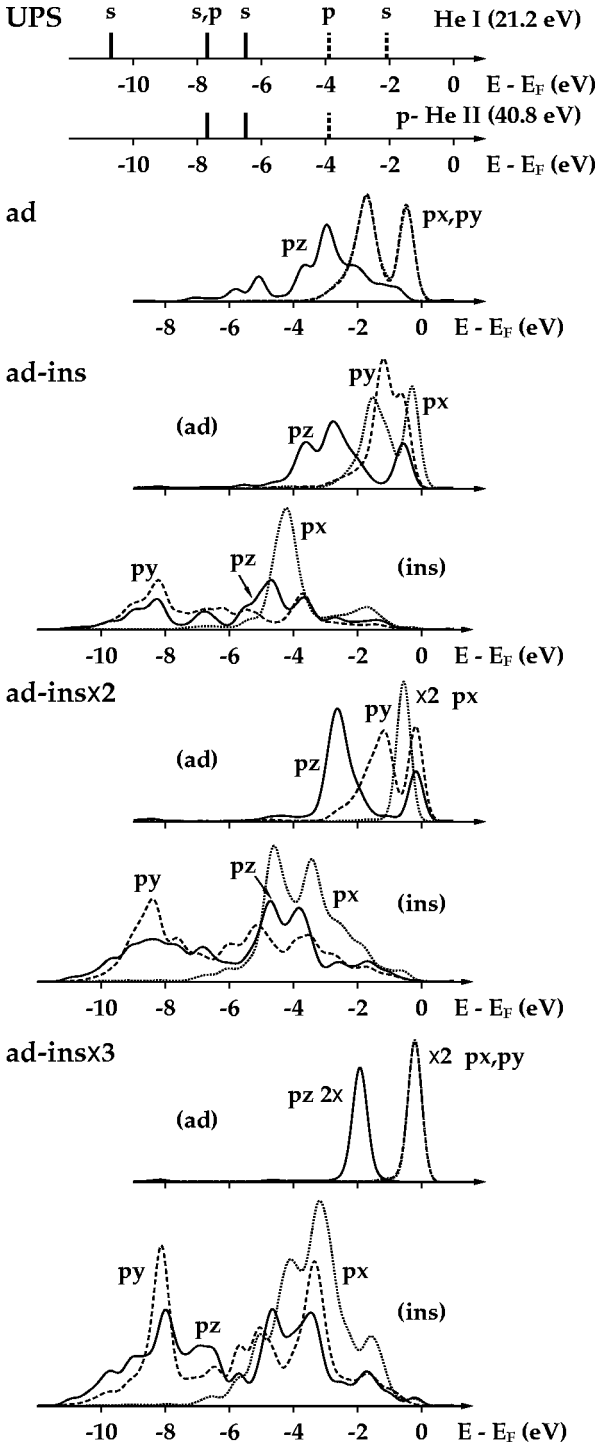

FIG. 3. PDOS of the oxygen $2p$ orbitals in the ad-ins$\times n$ models.The UPS spectra obtained by two different light sources (Höfer *et al.*, Ref. 2) are also given for comparison, where the *s* (*p*) labeled peaks are more prominent by *s*-polarized (*p*-polarized) light and the peaks drawn by a dashed line are metastable ones (see text). Note that the *z* axis is surface normal and the *x* axis is normal to the Si-O-Si plane, and the label ''$\times 2$'' indicates that the labeled peak is actually twice larger.

$$\frac{\partial^2 E_0}{\partial x_i \partial x_j} x_j^{\omega} = m_i \delta_{ij} \omega^2 x_j^{\omega}, \tag{3}$$

where E_0 is the total energy of the system, x_i's are the ionic displacements from the equilibrium positions, m_i is the ionic mass associated with the ith degree of freedom, and x_i^{ω}'s represent the normal mode with a vibrational frequency of ω. The derivative $\partial^2 E_0/\partial x_i \partial x_j = -\partial F_i/\partial x_j$, where F_i is the force acting on x_i, was calculated using a symmetric two-point finite difference formula with a displacement of ± 0.05 Å. We included in the calculation all the O atoms, the Si adatom, and the three first-layer Si atoms bonding with the adatom.

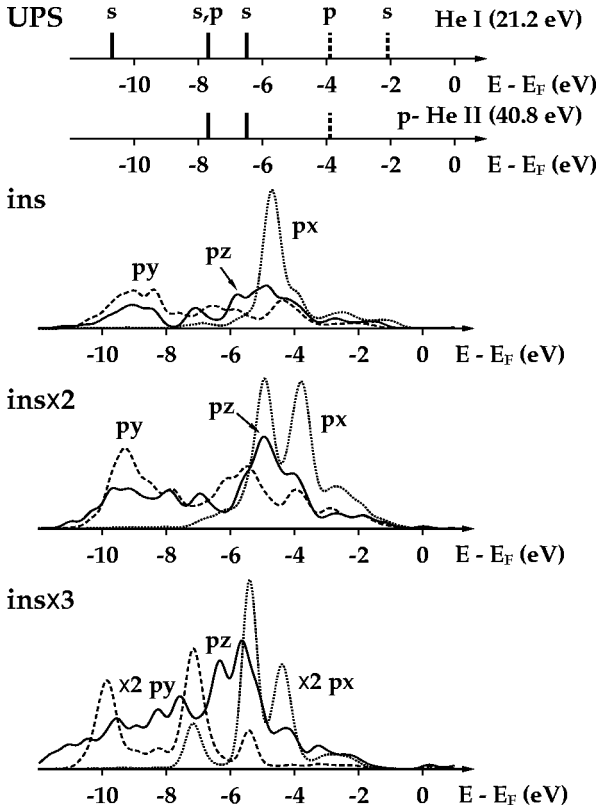

FIG. 4. PDOS of the oxygen $2p$ orbitals in the ins$\times n$ models.

We display in Fig. 5 the calculated vibration modes for each model in comparison with vibrational EELS data.[4,6,5,18] The EELS experiments observed that the 149–155 meV loss peak and other loss peaks at 85–130 meV show quite distinct thermal stability, i.e., the former disappears at $\sim$400 K and the latter is stable up to 600 K. In the calculations, the prominent, high-frequency modes are all oxygen related: the Si-O(ad) stretching mode has vibration frequencies of 136–143 meV, and the symmetric and asymmetric Si-O(ins)-Si stretching modes have 70-120 meV. The models with multiple O(ins) atoms exhibit splittings of the Si-O-Si stretching frequencies. Si related frequencies (not shown) are all below 55 meV.

By comparison with the EELS data, we can identify the O(ad) atoms as the origin of the metastable 149–155 meV loss peak and the O(ins) atoms, the stable loss peaks scattered over 85–130 meV. The underestimation of $\sim$10 meV seems to be a systematic error in the present scheme: Our calculation similarly underestimates the vibration frequency of a free SiO molecule, i.e., the calculated and experimental values are 148 and 154 meV, respectively.

In summary, the present vibrational analysis together with the PDOS analysis indicates unambiguously that any O(ad) atoms can produce the metastable features in UPS and EELS

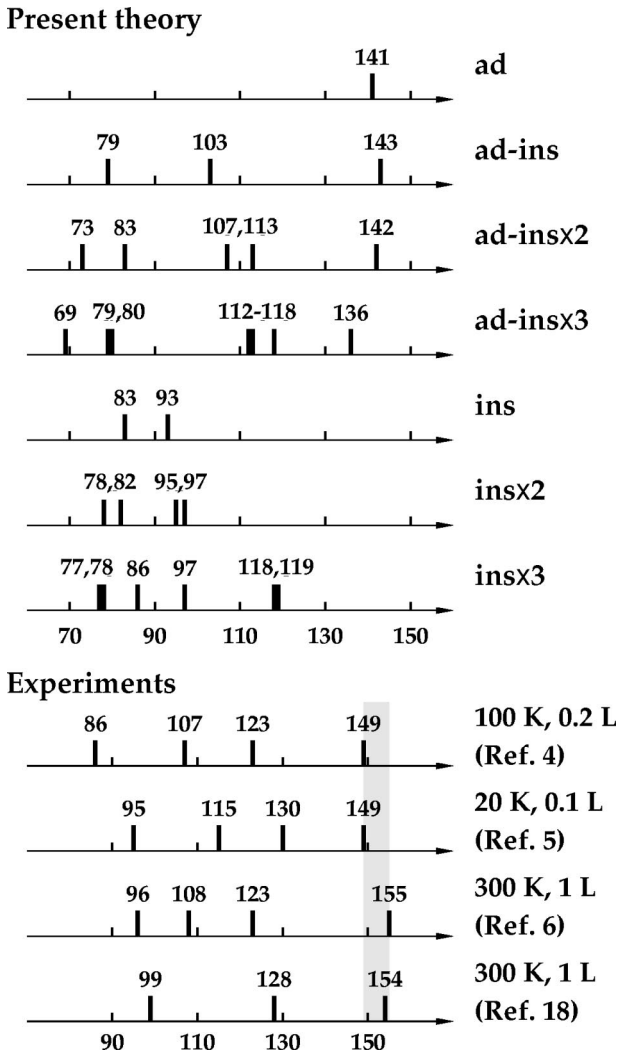

FIG. 5. Calculated vibration frequencies in comparison with EELS data. The gray region in the EELS data indicates the metastable loss peaks.

spectra, and that any O(ins) atoms are compatible with the stable features. Hence, the previous assignment of the metastable adsorption species to the ad-ins structure in Ref. 24 should be extended: Any of the ad-ins$\times n$ structures with $n=0$, 1, 2, or 3 can be a candidate for the metastable species.

D. Decay pathways

The present study has shown that all ad-ins$\times n$ structures can account for the metastable UPS and EELS features. In this section we discuss possible decay pathways of the metastable ad-ins$\times n$ structures.

Since the O(ins) configuration is the most stable for the adsorption of a single O atom,[38] the common picture of the decay of the metastable structures is an insertion of the O(ad) atom into one of the intact adatom backbonds. In this way, the metastable ad, ad-ins, and ad-ins$\times 2$ structures decay into the ins, ins$\times 2$, and ins$\times 3$ structures, respectively, and the energy gains obtained by the transformations amount to 1.2–1.3 eV (see Table III). The activation barrier for the ad-ins to ins$\times 2$ transition was calculated to be about 0.15 eV.[24] Similar barrier heights are expected for the other transitions with similar decay paths.

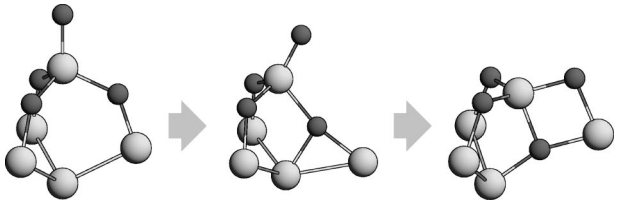

FIG. 6. Decay path of the ad-ins$\times 3$ structure.

The decay path of the ad-ins$\times 3$ structure is not so simple, since all the three back bonds are already filled with O(ins) atoms. The O(ad) atom can possibly hop first on top of a nearest restatom and then into a back-bond site of another adatom. Due to a large separation between the adatom and restatom sites, however, the calculated activation barrier for the first hopping is about 2.7 eV, too large to be related with the metastability at $\sim$400 K. We found an interesting decay path with a much lower activation barrier, as depicted in Fig. 6. Along this path, one of O(ins) atoms is pushed into the hollow region below the adatom, and successively the O(ad) atom decays into the ins site. The involved activation barrier is only 1.25 eV. The final structure, with a subsurface O atom bonding with three Si atoms, is 0.4 eV more stable than the ad-ins$\times 3$ structure. A similar threefold-coordinated oxygen configuration was also reported as a transient structure in the oxygen diffusion process in a previous molecular-dynamics study of the Si-SiO_2 interface.[39] This subsurface oxygen configuration therefore is likely a precursor state to the oxygen diffusion into the deeper layers.

The present finding of the two distinct decay energetics can be used to further narrow down the candidates for the metastable UPS and EELS features. When using the usual attempt frequency of 10^{14} s^{-1}, the Arrhenius law predicts that the ad-ins$\times 3$ structure, with its activation barrier of $\sim$1.25 eV, decays at $\sim$450 K, whereas the other ad, ad-ins, and ad-ins$\times 2$ structures decay at a much lower temperature ($\sim$50 K). In that case, the ad-ins$\times 3$ structure would be the only candidate for the metastable experimental features. However, it is not clear yet whether we can apply the usual attempt frequency to this system. For instance, x-ray photoemission and optical measurements[2,14] estimated the activation barrier as $\sim$0.2 eV with use of an extremely low attempt frequency of ~ 10 s^{-1}. A more conclusive identification is subject to experimental refinements.

IV. SUMMARY

The present DFT calculations have provided the energetics and the electronic and vibrational properties of all the possible dissociative oxidation configurations of the most reactive Si adatom site on Si(111)-(7$\times$7), the unit components of which are the O(ad) atoms bonding on top of the adatom and the O(ins) atoms inserted into the adatom back bonds. In energetics, we found that the O(ad) atoms are always less stable than the O(ins) atoms and determined the decay pathways of the metastable ad-ins$\times n$ (where $n=0$, 1, 2, or 3) structures, involving an O(ad)-to-O(ins) transition. We also found that the O(ad) atom of any ad-ins$\times n$ structures can produce the metastable UPS and EELS spectra and all O(ins) atoms, the stable UPS and EELS spectra. In

conclusion, all ad-ins$\times n$ (ins$\times n$) models are compatible, both energetically and spectroscopically, with the metastable (stable) experimental species. Our finding that the ad-ins $\times 3$ structure has an interesting decay mode distinguished from the ad, ad-ins, and ad-ins$\times 2$ structures will be useful in future studies to narrow down the candidates for the experimental metastable structures.

Note added in proof. We have recently examined the atomic origin of metastable oxygen 1*s* core-level peaks observed at this system. Our analysis leads to a conclusive identification of the long-sought metastable oxidation species as the ad-ins$\times 3$ structure.[40]

ACKNOWLEDGMENTS

This work was supported by the Korea Ministry of Education (Contract No. BSRI-98-2440) and the Korea Science and Engineering Foundation through the ASSRC at Yonsei University. We acknowledge helpful communications with I. W. Lyo and C. N. Whang.

[1] See, for example, T. Engel, Surf. Sci. Rep. **18**, 91 (1993).
[2] U. Höfer, P. Morgen, W. Wurth, and E. Umbach, Phys. Rev. Lett. **55**, 2979 (1985); Phys. Rev. B **40**, 1130 (1989).
[3] P. Morgen, U. Höfer, W. Wurth, and E. Umbach, Phys. Rev. B **39**, 3720 (1989).
[4] H. Ibach, H.D. Bruchmann, and H. Wagner, Appl. Phys. A: Solids Surf. **29**, 113 (1982).
[5] A.J. Schell-Sorokin and J.E. Demuth, Surf. Sci. **157**, 273 (1985).
[6] K. Edamoto, Y. Kubota, H. Kobayashi, M. Onchi, and M. Nishijima, J. Chem. Phys. **83**, 428 (1985).
[7] G. Dujardin, A. Mayne, G. Comtet, L. Hellner, M. Jamet, E. Le Goff, and P. Miller, Phys. Rev. Lett. **76**, 3782 (1996).
[8] I.-S. Hwang, R.-L. Lo, and T.T. Tsong, Phys. Rev. Lett. **78**, 4797 (1997).
[9] R. Martel, Ph. Avouris, and I.-W. Lyo, Science **272**, 385 (1996).
[10] I.-W. Lyo, Ph. Avouris, B. Schubert, and R. Hoffmann, J. Phys. Chem. **94**, 4400 (1990).
[11] J.P. Pelz and R.H. Koch, Phys. Rev. B **42**, 3761 (1990); **9**, 775 (1991).
[12] Ph. Avouris, I.-W. Lyo, and F. Bozso, J. Vac. Sci. Technol. B **9**, 424 (1991).
[13] F. Bozso and Ph. Avouris, Phys. Rev. B **44**, 9129 (1991).
[14] P. Bratu, K.L. Kompa, and U. Höfer, Phys. Rev. B **49**, 14 070 (1994).
[15] G. Dujardin, G. Comtet, L. Hellner, T. Hirayama, M. Rose, L. Philippe, and M.J. Besnard-Ramage, Phys. Rev. Lett. **73**, 1727 (1994).
[16] J.M. Seo, K.J. Kim, H.W. Yeom, and Ch. Park, J. Vac. Sci. Technol. A **12**, 2255 (1994).
[17] B. Lamontagne, D. Roy, R. Sporken, and R. Caudano, Prog. Surf. Sci. **50**, 315 (1995).
[18] K. Sakamoto, S. Suto, and W. Uchida, Surf. Sci. **357-358**, 514 (1996).
[19] J.S. Ha, K.-H. Park, E.-H. Lee, and S.-J. Park, Appl. Surf. Sci. **126**, 317 (1998).
[20] W.A. Goddard III, A. Redondo, and T.C. McGill, Solid State Commun. **18**, 981 (1976).
[21] M. Chen, I.P. Batra, and C.R. Brundle, J. Vac. Sci. Technol. **16**, 1216 (1979).
[22] S. Ciraci, Ş. Ellialtioğlu, and Ş. Erkoç, Phys. Rev. B **26**, 5716 (1982).
[23] B. Schubert, Ph. Avouris, and R. Hoffmann, J. Chem. Phys. **98**, 7593 (1993); **98**, 7606 (1993).
[24] S.H. Lee and M.H. Kang, Phys. Rev. Lett. **82**, 968 (1999).
[25] K.-Y. Kim, T.-H. Shin, S.-J. Han, and H. Kang, Phys. Rev. Lett. **82**, 1329 (1999).
[26] K.D. Brommer, M. Galván, A. Dal Pino,Jr. and J.D. Joannopoulos, Surf. Sci. **314**, 57 (1994).
[27] The two adatoms in the (4×2) unit cell are not equivalent: One has one nearest restatom site, while the other has two. In this study the former adatom site is used as the oxygen adsorption site.
[28] A. Vittadini and A. Selloni, Phys. Rev. Lett. **75**, 4756 (1995).
[29] In fact, we extended our search for the possibility of molecular configurations but found no (meta)stable molecular chemisorption species up to the second O_2 adsorption on the adatom site.
[30] The energy barrier for the abstractive adsorption of O_2 was found to be 0.8 eV on the unreacted adatom site and 0.4 eV on the ins$\times 2$ site. With an extended unit cell of (4×4), the barrier reduces to 0.4 eV and 0.15 eV, respectively.
[31] J.P. Perdew, K. Burke, and M. Ernzerhof, Phys. Rev. Lett. **77**, 3865 (1996).
[32] N. Troullier and J.L. Martins, Phys. Rev. B **43**, 1993 (1991).
[33] L. Kleinman and D.M. Bylander, Phys. Rev. Lett. **48**, 1425 (1982).
[34] The cutoff radii for the Si pseudopotential were taken at 1.55, 1.84, and 1.99 a.u. for *s*, *p*, and *d* angular-momentum components, respectively, where the *p* component was taken as the local potential. We used for hydrogen only the local *s* potential with a cutoff radius of 1.32 a.u.
[35] D. Vanderbilt, Phys. Rev. B **41**, 7892 (1990); K. Laasonen, A. Pasquarello, R. Car, C. Lee, and D. Vanderbilt, *ibid.* **47**, 10 142 (1993).
[36] Two reference energies corresponding to the *s* and *p* eigenvalues were used for both *s* and *p* angular-momentum components. The cutoff radii were taken at 1.5 a.u. for the valence electronic wave functions, 1.2 a.u. for the local potential, and 1.0 a.u. for the charge augmentation function.
[37] X. Blase, X. Zhu, and S.G. Louie, Phys. Rev. B **49**, 4973 (1994).
[38] For a single O atom, we found that bulk Si-Si bond sites or the hollow site below the adatom are less stable than the ins configuration by 1.4–1.6 eV.
[39] A. Pasquarello, M.S. Hybertsen, and R. Car, Nature (London) **396**, 58 (1998).
[40] S. H. Lee and M. H. Kang, Phys. Rev. Lett. **84**, 1724 (2000).